

Noise correlation and decorrelation in arrays of bolometric detectors

C. Mancini-Terracciano^{a,1} and M. Vignati^{a*}

*^aDipartimento di Fisica, Sapienza Università di Roma and Sezione INFN di Roma,
Piazzale A. Moro 2, Roma I-00185, Italy*

*¹now at Dipartimento di Fisica, Università degli Studi Roma Tre,
Via della Vasca Navale 84, Roma I-00146, Italy
E-mail:marco.vignati@roma1.infn.it*

ABSTRACT: Bolometers are phonon mediated detectors used in particle physics experiments to search for rare processes, such as neutrinoless double beta decay and dark matter interactions. They feature an excellent energy resolution, which is a few keV over an energy range extending from a few keV up to several MeV. Nevertheless the resolution can be limited by the noise induced by vibrations of the mechanical apparatus. In arrays of bolometers part of this noise is correlated among different detectors and can be removed using a multichannel decorrelation algorithm. In this paper we present a decorrelation method and its application to data from the CUORICINO experiment, an array of 62 TeO₂ bolometers.

KEYWORDS: Bolometers, Thermal noise, Digital signal processing.

*Corresponding author.

Contents

1. Introduction	1
2. Experimental setup	2
3. Noise correlation	3
4. Noise decorrelation	5
5. Application to data	7
6. Combination with the optimum filter	8
7. Conclusions	9

1. Introduction

Bolometers are detectors in which the energy from particle interactions is converted to thermal energy and measured via their rise in temperature. They provide excellent energy resolution, though their response is slow compared to conventional detectors. These features make them a suitable choice for experiments searching for rare processes, such as neutrinoless double beta decay (0 ν DBD) and dark matter (DM) interactions.

The CUORE experiment will search for 0 ν DBD of ^{130}Te [1, 2] using an array of 988 TeO_2 bolometers of 750 g each. Operated at a temperature of about 10 mK, these detectors feature an energy resolution of a few keV over their energy range, extending from a few keV up to several MeV. At low energies, below 100 keV, the resolution is of the order of 1 keV FWHM, while at 2528 keV, the 0 ν DBD energy, is about 5 keV FWHM; this, together with the low background and the high mass of the experiment, determines the sensitivity to the 0 ν DBD. CUORE could also search for DM interactions, provided that the energy threshold is of few keV [3]. An experiment made of 62 bolometers, CUORICINO [4], was operated at Laboratori Nazionali del Gran Sasso (LNGS) in Italy between 2003 and 2008, and proved the feasibility of the TeO_2 bolometric technique. CUORE is currently under construction, and will start taking data in three years.

Vibrations of the cryogenic apparatus (keeping the system at low temperatures) induce a visible noise, which limits the energy resolution at low energies [5] and the energy threshold [3]. Since all bolometers are held by the same structure, part of the vibrational noise is expected to be correlated.

In this paper we present a method to estimate the correlated noise among different bolometers, and a method to remove it. The application to data from CUORICINO shows that the correlated noise is visible and that it can be efficiently removed.

The CUORE detector structure will be different from the CUORICINO one, and thus a different vibrational noise is expected. If it will be unfortunately large, the algorithms developed in this work could be used to improve the performances of CUORE in both 0 ν DBD and DM searches.

2. Experimental setup

CUORICINO and CUORE bolometers are composed of two main parts, a TeO_2 crystal and a neutron transmutation doped Germanium (NTD-Ge) thermistor [6, 7]. The crystal is cube-shaped ($5 \times 5 \times 5 \text{ cm}^3$) and held by Teflon supports in copper frames. The frames are connected to the mixing chamber of a dilution refrigerator, which keeps the system at a temperature of about 10 mK. The thermistor is glued to the crystal and acts as thermometer. When energy is released in the crystal, its temperature increases and changes the resistance of the thermistor. To read out the signal, the thermistor is biased with constant current, which is provided by a voltage generator and a load resistor in series with the thermistor. The resistance of the thermistor varies in time with the temperature, and the voltage across it is the bolometer signal. The value of the load resistor is chosen to be much higher than the thermistor, so that the voltage across the thermistor is proportional to its resistance. The wires that connect the thermistor to the electronics introduce a non-negligible parasitic capacitance.

The typical response of CUORICINO and CUORE bolometers to particles impinging on the crystal is of order $100 \mu\text{V}/\text{MeV}$. The signal frequency bandwidth is 0 – 10 Hz, while the noise components extend to higher frequencies. The signal is amplified, filtered with a 6-pole active Bessel filter with a cut-off frequency of 12 Hz and then acquired with an 18-bit ADC with a sampling frequency of 125 Hz. The gain of the amplifiers ranges from 500 to 10000 V/V, and is tuned for each bolometer to fit the signals in the ADC range, which is $\pm 10.5 \text{ V}$. A typical signal recorded by the ADC, produced by a 1461 keV γ particle fully absorbed in a CUORICINO bolometer, is shown in the left panel of Fig. 1.

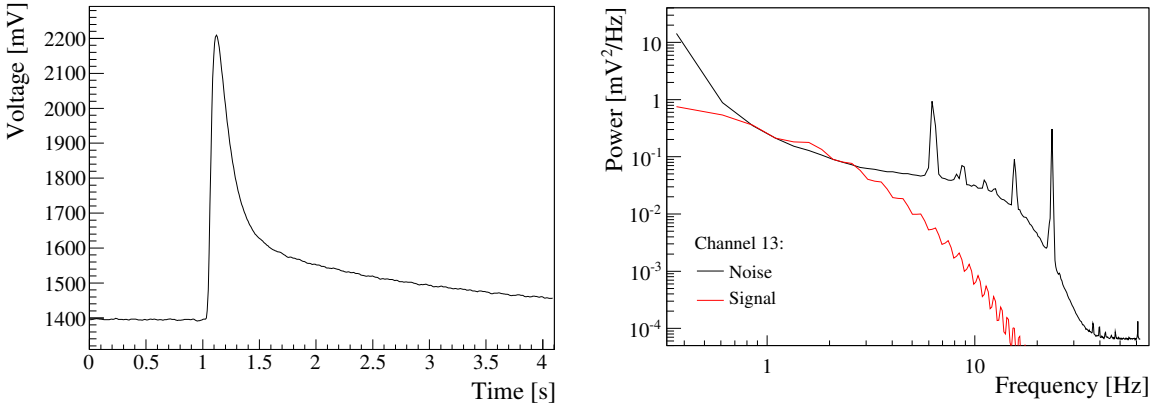


Figure 1. Response of a CUORICINO bolometer (channel 13). Left panel: signal generated by a 1461 keV γ particle recorded by the ADC. Right panel: noise power spectrum expressed in mV^2/Hz , and energy spectrum of the signal scaled to fit in the noise range.

The 62 bolometers of CUORICINO were arranged in a tower of 13 floors: 11 floors were composed by 4 $5 \times 5 \times 5 \text{ cm}^3$ bolometers each, 2 floors were composed by 9 small bolometers ($3 \times 3 \times 6 \text{ cm}^3$) each. The small bolometers were recycled from previous arrays, and will not be used in CUORE, which will only use $5 \times 5 \times 5 \text{ cm}^3$ crystals arranged in 19 towers of 13 floors each (Fig. 2). The front-end electronics, which provide the bias, the load resistors and the amplifier, are placed outside the cryostat, at room temperature [8]. In CUORICINO, 1/3 of the electronics channels used load resistors and pre-amplifiers located inside the cryostat, at 110 K. This was done to reduce the noise

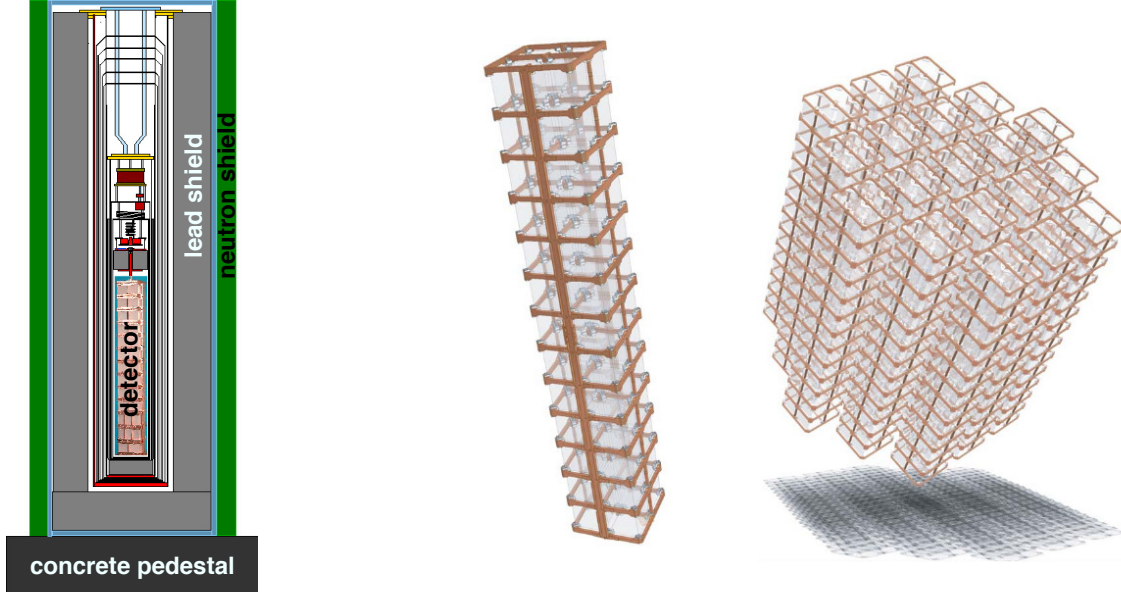


Figure 2. Arrays of TeO_2 bolometers. The CUORICINO tower (left), composed by 62 bolometers, represented inside a schema of the cryostat; a single CUORE tower (middle) and the entire CUORE array (right).

from load resistors, but since no improvement was achieved, the cold electronics will not be used in CUORE. Three channels (1 cold, 2 warm) were lost after the initial CUORICINO cool-down, reducing the number of active channels to 59.

Vibrations of the detector structure generate two types of noise: thermal and microphonic. The thermal noise is due to vibrations of the crystals that induce temperature fluctuations of the crystals themselves. The microphonic noise is due to vibrations of the wires that connect the thermistor to the cryostat socket. A typical noise power spectrum is shown in the right panel of Fig. 1; the peaks in the figure are attributed to microphonism, while the continuum is attributed to crystal vibrations.

The data acquisition system connected to the ADC boards implements two kind of software triggers. The first trigger fires when a signal is detected on a bolometer, the second fires randomly in time to acquire noise waveforms. To estimate the noise correlation, the acquisition was programmed to acquire simultaneously all the bolometers of CUORICINO when the signal or the noise triggers fired on a bolometer. The length of the acquisition window was set to $M = 512$ samples on all channels, corresponding to 4.096 s. The data used in this paper amount to 2 days taken from the last month of CUORICINO operation.

3. Noise correlation

The noise power spectrum is estimated from a large number of waveforms acquired with the random trigger, removing those that, by chance, contain signals. The power spectrum $N_i(\omega)$ of each bolometer channel i is computed as:

$$N_i(\omega) = \langle n_i(\omega) \cdot n_i^*(\omega) \rangle, \quad (3.1)$$

where $\langle \rangle$ denotes the average taken over a large number of waveforms and $n(\omega)$ is the discrete Fourier transform (DFT) of a noise waveform $n_i(t)$. To avoid DFT artifacts, each waveform is weighted before the DFT using a Welch windowing function:

$$n_i(t) \rightarrow n_i(t) \cdot w(t), \quad w(t) = \frac{1}{G} \left\{ \frac{M}{2} - \left[\left(t - \frac{M}{2} \right) \right]^2 \right\}. \quad (3.2)$$

In the above expression the parameter G is a normalization coefficient chosen to satisfy the condition [9]:

$$\sum_{\omega} N_i(\omega) = \sigma_i^2 \quad (3.3)$$

where σ_i is the standard deviation of the noise in the time domain.

The covariance between the noises on bolometers channels i and j is estimated as:

$$N_{ij}(\omega) = \langle n_i(\omega) \cdot n_j^*(\omega) \rangle \quad (3.4)$$

where the definitions are the same of Eq. 3.1. The magnitude of $N_{ij}(\omega)$ is the covariance as usually intended for real variables, while the phase accounts for any possible time delay of the frequency ω observed in the two bolometers. The correlation is also a complex quantity, and is defined as:

$$\rho_{ij}(\omega) = \frac{N_{ij}(\omega)}{\sqrt{N_i(\omega)N_j(\omega)}}. \quad (3.5)$$

As an example, we show the behaviour of $\rho_{13,1}(\omega)$ in Fig. 3; the microfonic peaks and the low frequencies are highly correlated, while the intermediate frequencies are almost uncorrelated. The pattern in the figure is visible for many (i, j) pairs and indicates that the source of correlated noise has analogous origin in all bolometers.

The average correlation over all frequencies can be computed as:

$$\overline{\rho_{ij}} = \sqrt{\frac{\sum_{\omega} |\rho_{ij}(\omega)|^2 N_i(\omega)}{\sum_{\omega} N_i(\omega)}}, \quad (3.6)$$

and is found to be around 60% for the (i, j) pair (13, 1). The average correlation matrix, including the correlation of all the CUORICINO channels, is shown in Fig. 4. The matrix is not exactly triangular because Eq. 3.6 is not symmetric under the exchange of channels i and j , since the same frequency may contribute with a different weight to $N_i(\omega)$ and $N_j(\omega)$. The figure shows that the correlation is high, even though there is no evident link with the spatial disposition of the bolometers. Bolometers close to each other, in fact, are not necessarily the most correlated.

We also tried to order the channels by their cabling group in the cryostat or by cold/warm electronics channels, but also in this case we did not see any link. Other variables linked to the noise correlation could be, for example, the path of the wires along the tower, the tightness of the crystals and the length of thermistor wires. These variables are not accessible now since CUORICINO has been disassembled. Moreover, while the understanding of the noise sources is important, in this paper we focus on the analysis algorithms to reduce the observed noise.

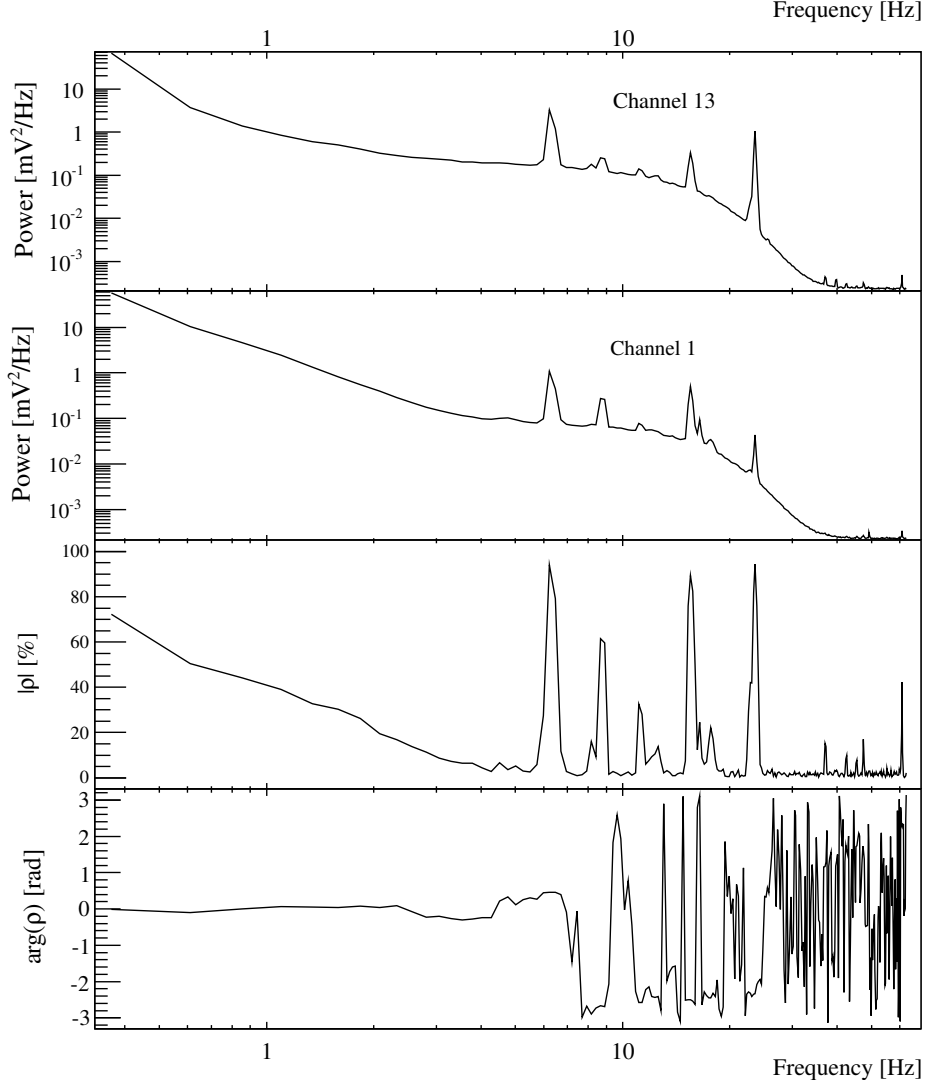


Figure 3. Power spectra of CUORICINO channels 13 and 1 and their correlation $\rho(\omega)$.

4. Noise decorrelation

In TeO_2 bolometers the noise is purely additive to the signal, meaning that the waveform $f(t)$ observed in presence of a signal of amplitude A can be expressed as:

$$f(t) = A \cdot s(t) + n(t) , \quad (4.1)$$

where $s(t)$ is the signal shape. Since the noise on different bolometers is partially correlated, it is possible to remove part of $n(t)$ from $f(t)$ using the waveforms from other bolometers in which only noise is present. In the following we develop a method to remove the correlated noise.

Assuming that each frequency component of $n_i(\omega)$ is normally distributed, the multidimensional probability distribution of the noises on all bolometers $\vec{n}(\omega) = \{n_1(\omega), n_2(\omega), \dots\}$ can be

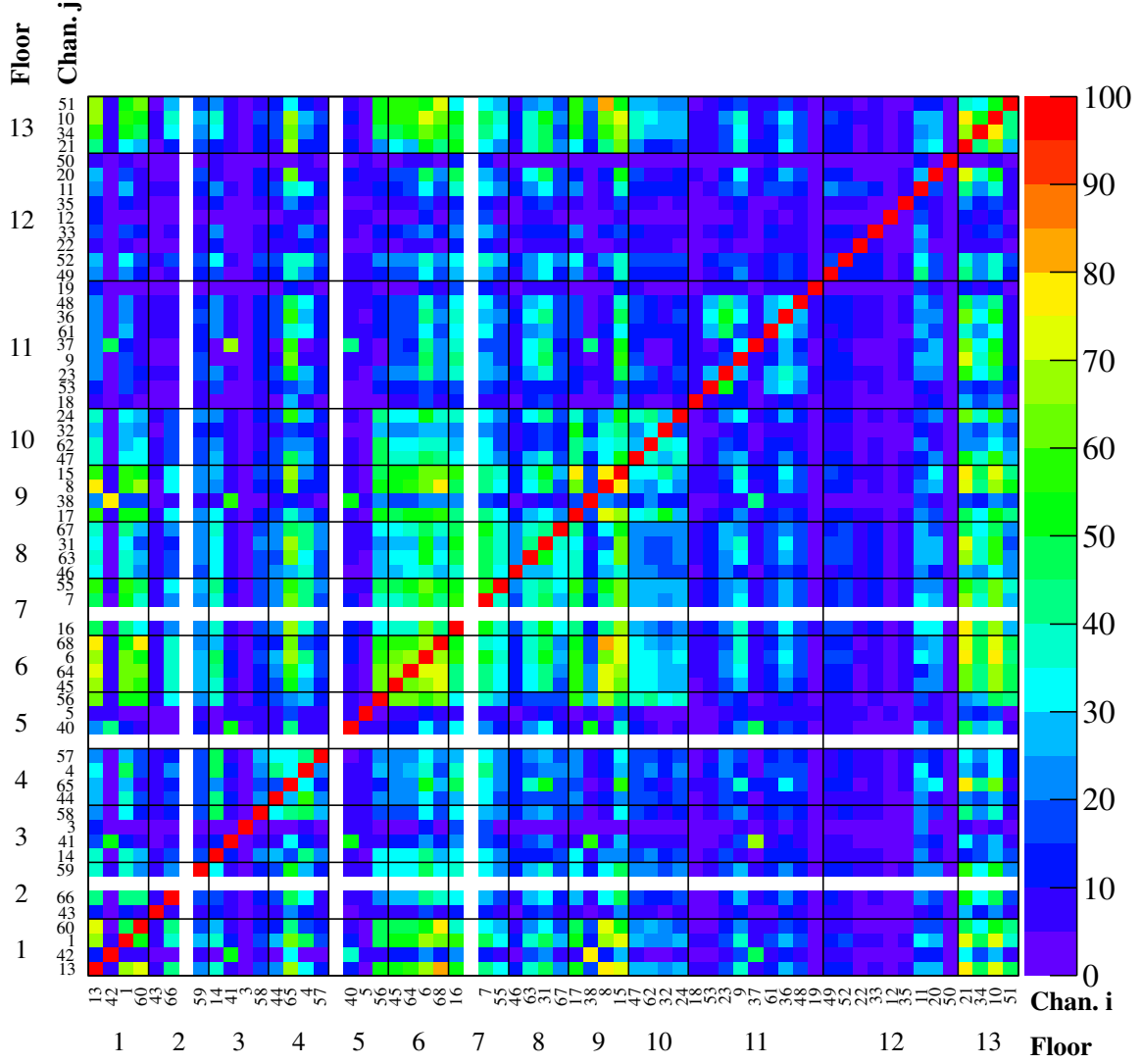


Figure 4. Noise correlation in CUORICINO. Channels are ordered as bolometers are ordered in the array. White lines indicate dead channels.

written as:

$$P[\vec{n}(\omega)] \propto \exp\left(-\frac{1}{2}\vec{n}^\dagger(\omega)\hat{N}^{-1}(\omega)\vec{n}(\omega)\right) \quad (4.2)$$

where \hat{N} is the covariance matrix whose elements are defined in Eq. 3.4. The probability distribution of the noise on bolometer i , $n_i(\omega)$, can be obtained integrating out the noise of other bolometers:

$$P[n_i(\omega)] \propto \exp\left[-\frac{N_{ii}^{-1}(\omega)}{2}\left(n_i(\omega) + \sum_{j \neq i} \frac{N_{ij}^{-1}(\omega)}{N_{ii}^{-1}(\omega)} n_j(\omega)\right)^2\right]. \quad (4.3)$$

The above equation represents a Gaussian with mean $\left[-\sum_{j \neq i} \frac{N_{ij}^{-1}(\omega)}{N_{ii}^{-1}(\omega)} n_j(\omega)\right]$ and variance $1/N_{ii}^{-1}(\omega)$.

The decorrelated value of $n_i(\omega)$ can be obtained for each waveform as:

$$n_i^d(\omega) = n_i(\omega) + \sum_{j \neq i} \frac{N_{ij}^{-1}(\omega)}{N_{ii}^{-1}(\omega)} n_j(\omega), \quad (4.4)$$

and its power spectrum is expected to be:

$$N_i^d(\omega) = \frac{1}{N_{ii}^{-1}(\omega)}. \quad (4.5)$$

A generic waveform $f_i(t)$ on bolometer i , containing noise or noise+signal, can be decorrelated using the noise from all other bolometers as:

$$f_i^d(\omega) = f_i(\omega) + \sum_{j \neq i} \frac{N_{ij}^{-1}(\omega)}{N_{ii}^{-1}(\omega)} n_j(\omega) = A s_i(\omega) + n_i^d(\omega). \quad (4.6)$$

Summarizing, once the covariance matrix in Eq. 3.4 is estimated from the data, the waveforms on each bolometer are decorrelated using Eq. 4.6 and the effect on the noise power spectrum can be predicted with Eq. 4.5.

5. Application to data

The acquired data are split in two sets, one set is used to estimate the correlation matrix and the expected noise power spectra, the other is used to verify that the application of the decorrelation algorithm to waveforms produces results consistent with the expectations. Figure 5 (left) shows the original power spectrum of channel 13 (Eq. 3.1) and the one expected decorrelating from all the other CUORICINO bolometers (Eq. 4.5). The power of low frequencies is reduced and the microphonic peaks are completely removed. In principle one could be satisfied and proceed to apply Eq. 4.6 to the single waveforms. However, using all the bolometers to decorrelate every triggered waveform is expensive from the computational point of view, since it requires DFTs for each bolometer used. Moreover all the waveforms used to decorrelate should not contain signals. This requirement is often fulfilled in CUORICINO, where the overall counting rate was around 0.1 Hz, but not in CUORE, where the rate is expected to be larger. For this reason we tested to see if the decorrelation is effective using a smaller number of bolometers. For each bolometer we selected the most correlated bolometers and we computed the expected decorrelated power spectrum. The results obtained are equivalent to those obtained using all bolometers (Fig. 5 left). The number of bolometers used to decorrelate was set to 11, a number sufficiently high to maximize the decorrelation and sufficiently low to ensure good performances.

The noise power spectrum obtained on waveforms decorrelated with Eq. 4.6 is shown in Fig. 5 (right). The decorrelation is found to be very effective on channel 13: the noise σ is reduced from 2.0 mV to 1.2 mV (corresponding to 3.6 and 2.2 keV, respectively), an effect which is visible also in the time domain (Fig. 6). We show in Fig. 7 the energy resolution on all bolometers before and after the decorrelation: in a few bolometers the resolution remains the same, while in others it is reduced up to 50%.

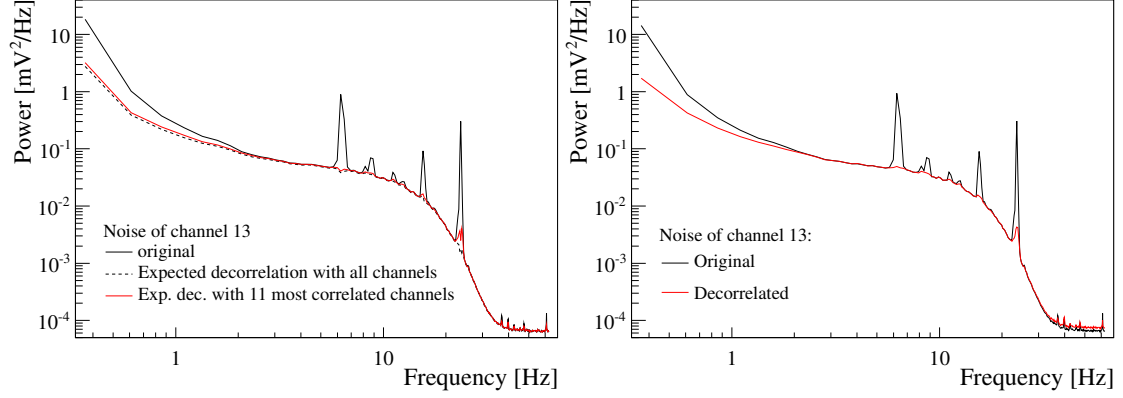


Figure 5. Left: Noise power spectra of bolometer 13: original (solid black), expected decorrelated using 61 bolometers (dashed black), and expected decorrelated using the 11 most correlated bolometers (solid red). Right: original noise power spectrum and power spectrum of waveforms decorrelated using Eq. 4.6. The original power spectra in the figures differs slightly because different sets of data has been used to estimate the covariance matrix (left) and the effect of the decorrelation (right).

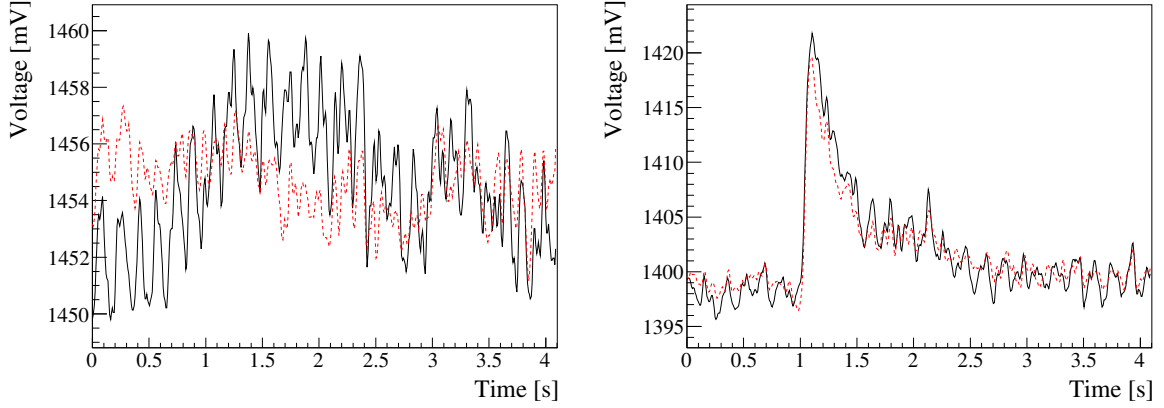


Figure 6. Left: original (solid black) and decorrelated (dashed red) noise waveform from channel 13. Right: signal generated by a 43 keV γ particle. The decorrelation algorithm reduces the noise leaving the signal unmodified.

6. Combination with the optimum filter

In the data analysis of TeO_2 bolometers the signal amplitude is estimated using the optimum filter [10, 11], a filter that significantly improves the energy resolution. This filter can be used when the shape of the signal and the noise power spectrum of each channel are known. The filter acts on a single channel and its transfer function is

$$H(\omega) = h \frac{s^*(\omega)}{N(\omega)} e^{-j\omega i_M}, \quad (6.1)$$

where i_M is a parameter to adjust the delay of the filter. In this work, as in Ref. [3], we chose it equal to the maximum position of s_i , so that the maximum of the filtered signal is aligned to

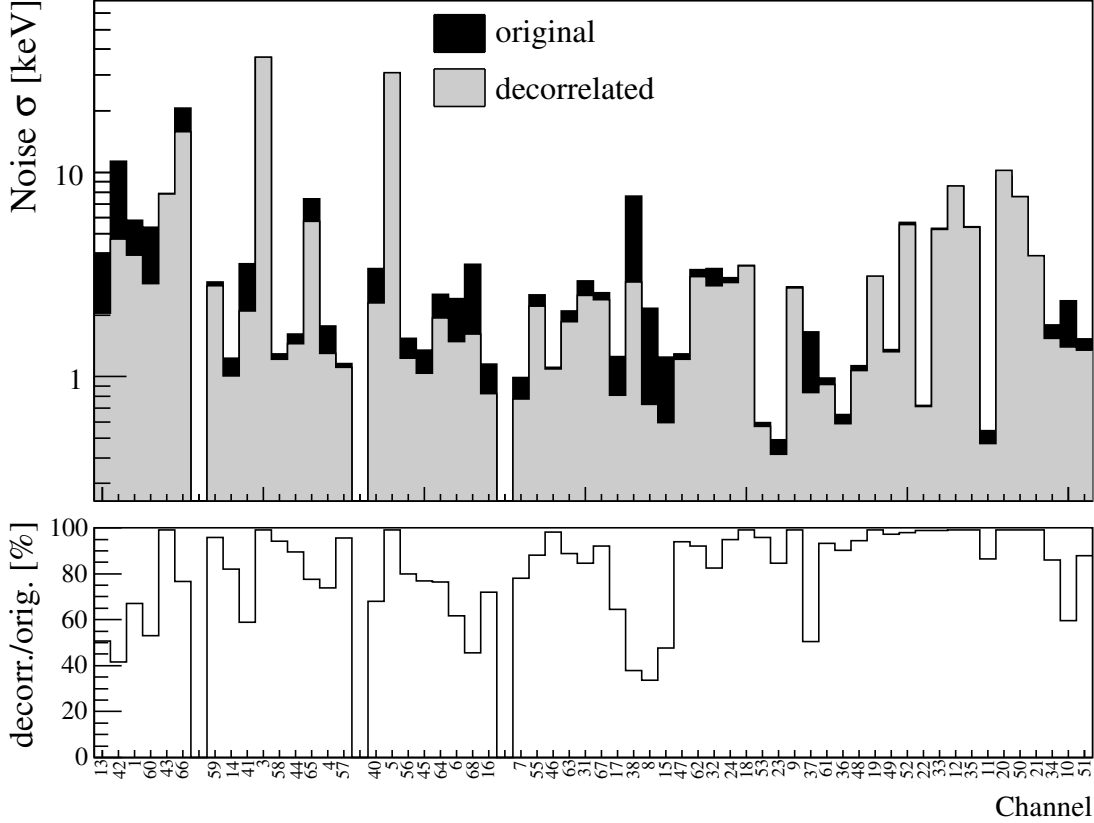


Figure 7. Noise resolution of all CUORICINO bolometers before and after the decorrelation. Values are expressed in keV.

the maximum of the non-filtered one. h is a normalization constant that leaves unmodified the amplitude of the signal: $h = \left[\sum_{\omega} \frac{|s(\omega)|^2}{N(\omega)} \right]^{-1}$.

To combine the optimum filter with the decorrelation, it is sufficient to replace in Eq. 6.1 the original power spectrum $N(\omega)$ with $N^d(\omega)$ defined in Eq. 4.5, and then process the decorrelated waveforms in Eq. 4.6. The comparison of the filtered noise power spectrum with and without the decorrelation for two bolometers with opposite behavior (channels 13 and 38) is shown in Fig. 8. In channel 13, while the decorrelated noise is lower than the original one, there is no big improvement in the filtered-decorrelated noise, because the correlation is high only on frequencies with low signal to noise ratio. In channel 38, on the other hand, the decorrelation lowers the noise after the optimum filter.

To summarize we compare the expected resolution of the entire array using both decorrelation and optimum filter with respect to optimum filter only (Fig. 9). The improvement is not significant as when we decorrelated the original waveforms (Fig. 7), because in most cases the noise is not correlated in the signal frequency bandwidth.

7. Conclusions

In this paper we developed a method to remove the correlated noise between different detectors.

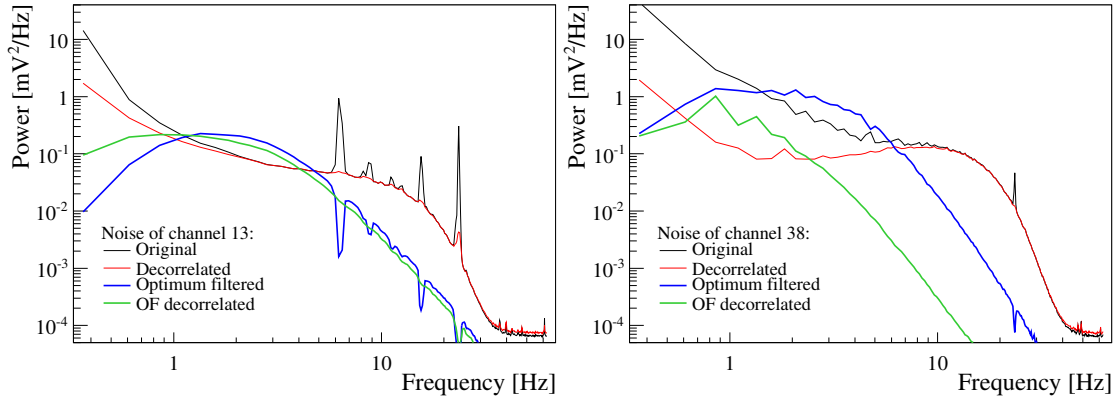


Figure 8. Comparison of original, decorrelated, optimum filtered and decorrelated/optimum filtered noises on bolometers 13 (left) and 38 (right).

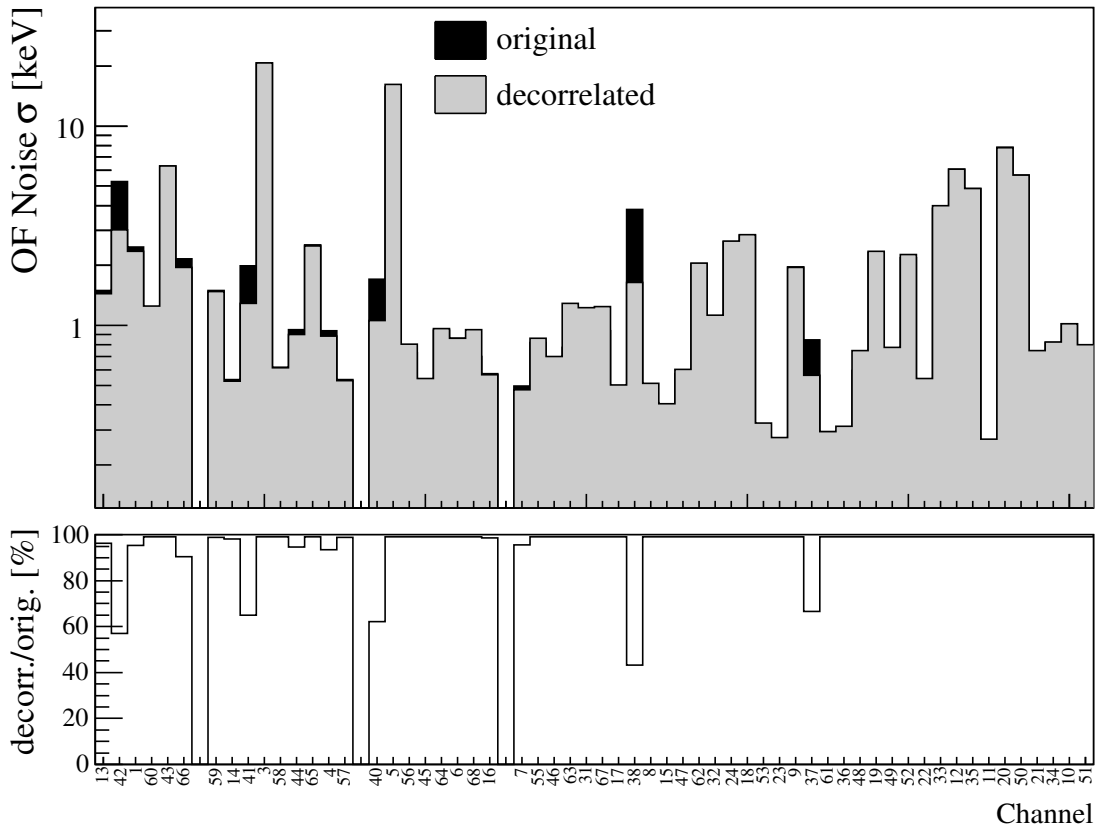


Figure 9. Noise resolution of all CUORICINO bolometers after the optimum filter before and after the decorrelation.

The application to CUORICINO showed that the correlated noise, generated by vibrations of the detector structure, can be efficiently removed. However, when the decorrelation is combined with the optimum filter, the resolution does not improve significantly since the correlated noise lies at frequencies higher than the signal frequency bandwidth. CUORE, a TeO₂ bolometric array 20 times

larger than CUORICINO, will have a new detector structure that could induce different vibrational noise. Moreover, while CUORICINO was refrigerated using liquid helium, the CUORE cryostat will use pulse tubes, acoustic cryocoolers oscillating at low frequencies (around 2 Hz). If the noise will be unfortunately large in the signal band, the method we introduced will be a valid tool to improve the CUORE performances.

Acknowledgments

We are very grateful to the members of the CUORICINO and CUORE collaborations, in particular to F. Bellini, L. Cardani, T. Gutierrez, K. Han and G. Pessina for their precious suggestions. Special thanks go to Robert Joachim, for the preliminary studies he did during his summer student fellowship at INFN Roma.

References

- [1] R. Ardito *et al.*, *CUORE: A Cryogenic Underground Observatory for Rare Events*, hep-ex/0501010.
- [2] C. Arnaboldi *et al.*, *CUORE: A Cryogenic Underground Observatory for Rare Events*, *Nucl. Instrum. Meth. A* **518** (2004) 775, [hep-ex/0212053v1].
- [3] S. Di Domizio, F. Orio, and M. Vignati, *Lowering the energy threshold of large-mass bolometric detectors*, *JINST* **6** (2011) P02007, [arXiv:1012.1263].
- [4] E. Andreotti *et al.*, *^{130}Te Neutrinoless Double-Beta Decay with CUORICINO*, *Astropart.Phys.* **34** (2011) 822, [arXiv:1012.3266].
- [5] F. Bellini *et al.*, *Response of a TeO_2 bolometer to alpha particles*, *JINST* **5** (2010) P12005, [arXiv:1010.2618].
- [6] N. Wang *et al.*, *Electrical and thermal properties of neutron-transmutation-doped Ge at 20 mK*, *Phys. Rev. B* **41** (1990) 3761.
- [7] K. M. Itoh *et al.*, *Neutron transmutation doping of isotopically engineered Ge*, *Appl. Phys. Lett.* **64** (1994) 2121.
- [8] C. Arnaboldi *et al.*, *The programmable front-end system for CUORICINO, an array of large-mass bolometers*, *IEEE Trans. Nucl. Sci.* **49** (2002) 2440.
- [9] M. Novotny and M. Sedlacek, *RMS value measurement based on classical and modified digital signal processing algorithms*, *Measurement* **41** (2008) 236.
- [10] E. Gatti and P. F. Manfredi, *Processing the signals from solid state detectors in elementary particle physics*, *Riv. Nuovo Cimento* **9** (1986) 1.
- [11] V. Radeka and N. Karlovac, *Least-square-error amplitude measurement of pulse signals in presence of noise*, *Nucl. Instrum. Methods* **52** (1967) 86.